

Unclas

00/47 0213102

NAG5-189

A STATISTICAL ANALYSIS OF THE MACROSCOPIC BEHAVIOR OF MOIST-CONVECTIVE PROCESSES

Jeng-Ming Chen and Akio Arakawa

Department of Atmospheric Sciences, University of California
Los Angeles, California 90024

1. INTRODUCTION

The heat sources in the atmosphere are primarily due to latent heat release within deep cumulus clouds and, therefore, they are not only the cause of the motion but a consequence of the motion as well. Understanding the nature of this coupling is crucial in parameterizing cumulus clouds, in which we attempt to quantitatively formulate the collective effects of subgrid-scale cumulus clouds in terms of the prognostic variables of resolvable scale.

While concentrating on the thermodynamical aspects of parameterizing deep cumulus clouds, Arakawa and Chen (1987) noted that the closure assumptions in the existing schemes are some combinations of the four types given below.

- Type I: Constraint on the coupling of net warming and net moistening by assuming the existence of equilibrium states.
- Type II: Constraint on the coupling of Q_1 (apparent heat source) and Q_2 (apparent moisture sink) through a cumulus ensemble model.
- Type III: Constraint on the coupling of cloud mass flux with the large-scale vertical mass flux at cloud base and/or the surface turbulent fluxes.
- Type IV: Constraints directly on the coupling of Q_1 and Q_2 with advective (and boundary-layer) processes.

In the Arakawa-Schubert scheme (Arakawa and Schubert, 1974), the type I closure is the equilibrium of cloud work function, $A(\lambda)$. Here λ is the fractional rate of entrainment, which is used as a parameter to identify cloud type, and $A(\lambda)$ is the work done by the buoyancy force per unit mass flux at cloud base. Following Arakawa and Schubert (1974), we can express the cloud work function as

$$A(\lambda) = \int_{z_B}^{\hat{z}(\lambda)} \beta(z) \left\{ L(q_S - q_S^*) + h_S^* - h_{B+}^* + \int_{z_{B+}}^z \eta(z', \lambda) \left[\lambda L(q(z') - q^*(z')) - \partial h^*(z') / \partial z' \right] dz' \right\} dz, \quad (1)$$

where z_B and $\hat{z}(\lambda)$ are the heights of cloud base and cloud top, q is the mixing ratio of water vapor, h is the moist static energy given by $c_p T + gz + Lq$, q^* is the saturation value of q , h^*

is the saturation moist static energy given by $c_p T + gz + Lq^*$, $\eta(z, \lambda)$ is the cloud mass flux normalized at cloud base, which satisfies $\partial \eta(z, \lambda) / \partial z = \lambda \eta(z, \lambda)$, the subscripts S and $B+$ denote an arbitrary level within the subcloud mixed layer and a level slightly above the mixed layer, respectively, $\beta \equiv g / c_p T(1 + \gamma)$, and $\gamma \equiv (L / c_p) (\partial q^* / \partial T)_p$. It should be noted that the type I closure in this scheme gives a constraint only on the coupling of the temperature and humidity profiles.

The cloud work function for the deepest clouds, for which $\lambda = 0$ and $\eta(z, \lambda) = 1$, becomes

$$A(0) = \int_{z_B}^{z_T} \beta(z) \left[L(q_S - q_S^*) - \int_{z_S}^z \frac{\partial h^*(z')}{\partial z'} dz' \right] dz \quad (2)$$

Here z_T is the height of the deepest cloud top. Since $\partial h^* / \partial z = -(1 + \gamma)(\Gamma - \Gamma_m)$, where Γ_m is the moist-adiabatic lapse rate, and $q_S - q_S^* = -(1 - RH_S)q^*$, where RH_S is the relative humidity at level S , the equilibrium $\partial A(0) / \partial t = 0$ means that for a fixed T_S , changes in RH_S and $\Gamma - \Gamma_m$ are negatively correlated if deep cumulus clouds exist.

The type II closure in the Arakawa-Schubert scheme is implicit in the use of a cumulus ensemble model, in which both Q_1 and Q_2 are expressed in terms of a single one-dimensional variable $M_B(\lambda)$, the cloud-base mass flux. Those expressions are

$$\rho Q_1 = -DL\hat{z} + M_C \partial s / \partial z, \quad (3)$$

$$-\rho Q_2 = DL(\hat{z} + q^* - q) + M_C L \partial q / \partial z. \quad (4)$$

Here $\hat{z}(z)$ is the liquid water mixing ratio of the cloud air that are detraining at level z ; $D(z)$ is the mass detrainment from clouds per unit height at level z , given by

$$D(z) = -M_B(\hat{\lambda}) \eta(z, \hat{\lambda}) d\hat{\lambda} / dz; \quad (5)$$

$M_B(\lambda) d\lambda$ is the cloud-base mass flux due to clouds whose fractional rate of entrainment is between λ and $\lambda + d\lambda$; $\hat{\lambda}(z)$ is λ of the clouds detraining at level z ; and $M_C(z)$ is the total cloud mass flux at level z , given by

$$M_C(z) = \int_0^{\lambda_{\max}} M_B(\lambda) \eta(z, \lambda) d\lambda, \quad (6)$$

where λ_{\max} is the maximum value of λ . The terms

involving M_C in (3) and (4) represent warming and drying of the environment through cloud-induced subsidence. Substituting (5) and (6) into (3) and (4) and eliminating $M_B(\lambda)$, we obtain integral relations that couple Q_1 and Q_2 . The relations may be formally written as

$$\int_z^{z_T} (F(z, z')Q_1(z') + G(z, z')Q_2(z'))dz' = 0 \quad (7)$$

for all $z < z_T$. For a layer in which the detrainment effects are negligible, (7) can be greatly simplified. Dropping the detrainment terms and eliminating M_C between (3) and (4), we obtain

$$Q_1/(\partial s/\partial z) - Q_2/(-L\partial q/\partial z) = 0. \quad (8)$$

2. PRELIMINARY RESULTS WITH LOW VERTICAL RESOLUTION

In the paper Arakawa and Chen (1987), we emphasized that observations should be used more extensively than in the past to directly verify and improve closure assumptions and to assess the limit of parameterizability. The paper presented preliminary results from an analysis of the macroscopic behavior of moist convection, which are summarized below.

The analysis was divided into two categories. To study type I closure, we analyzed a number of vertical profiles of temperature and humidity to find statistical constraints on their coupling under the existence of moist convection (type I coupling). To study type II closure, we analyzed a number of vertical profiles of Q_1 and Q_2 , which were obtained as residuals in the observed budgets, to find statistical constraints on their coupling (type II coupling). One of the principal datasets we used is the 3-hourly "GATE dataset", which is a subset of the gridded data for v , θ and q analyzed by Ooyama, Esbensen and Chu (see Esbensen and Ooyama, 1983). To obtain $Q_1 - Q_R$, where Q_R is the radiative heating rate, the gridded data for Q_R given by Cox and Griffith (1979) were used. Another principal dataset we used is the 12-hourly "Asian dataset", which is a subset of the gridded dataset analyzed by He et al. (1987) over Asia for the period of April 16 through July 4, 1979. The subset consists of data at 10 grid points over India and 14 grid points over eastern Asia mostly over China. No correction of Q_1 by Q_R was made for this dataset.

Before making a detailed statistical analysis, we performed a "quick-look" analysis of the two datasets. To see type I coupling, we plotted Γ_N vs. RH_S , where Γ_N is a normalized lapse rate given by $(\Gamma - \Gamma_{MS})/(\Gamma_d - \Gamma_{MS})$, Γ is the mean lapse between the surface and 500 mb, Γ_{MS} is the moist-adiabatic lapse rate at the surface and Γ_d is the dry-adiabatic lapse rate. A striking feature of these plots is the clustering of the points around the cloud work function equilibrium curve for deep clouds, showing a high negative correlation between Γ_N and RH_S . As anticipated, the scatter of the points are less in the plots for precipitating cases. To see type II coupling, we plotted \hat{Q}_1 vs. \hat{Q}_2 for each layer in the vertical, where

$$\begin{aligned} \hat{Q}_1 &\equiv Q_1(-L\partial q/\partial z)/(\partial s/\partial z)(-L\partial \bar{q}/\partial z), \\ \hat{Q}_2 &\equiv Q_2(\partial s/\partial z)/(\partial \bar{s}/\partial z)(-L\partial \bar{q}/\partial z), \end{aligned} \quad (9)$$

and the overbar denotes the time average. For the GATE dataset, $Q_1 - Q_R$ is used as Q_1 in (9). These plots show that $\hat{Q}_1 = \hat{Q}_2$ is a good first approximation. In view of (8), this suggests that subsidence between clouds is primarily responsible for Q_1 and Q_2 .

Encouraged by the results of the "quick-look" analysis, we studied the coupling between two variables in more detail. The method we have chosen is the canonical correlation analysis (see, for example, Cooley and Lohnes, 1971). In our application of this analysis, we consider a pair of two variables, X and Y , and treat their vertical profiles as vectors \mathbf{X} and \mathbf{Y} . Given a statistical sample of observed \mathbf{X} and \mathbf{Y} , we first remove the respective sample mean from each vector. We then consider linear transformations from \mathbf{X} to \mathbf{X}' and from \mathbf{Y} to \mathbf{Y}' . The transformations are chosen in such a way that each pair of the transformed components, (X'_1, Y'_1) , (X'_2, Y'_2) , ... has (locally) maximum correlation for the given sample. The (orthogonal) transformed components obtained in this way are the canonical components of \mathbf{X} and \mathbf{Y} . By examining the correlation and associated variances for each pair of the canonical components, we determine how strongly the vertical profiles of X and Y are coupled.

Type I coupling

For the canonical correlation analysis of type I coupling, Arakawa and Chen (1987) chose $-\partial h^*/\partial z$ and $L(q - q^*)$ of the Asia dataset as X and Y . This choice was guided by (1). The values of $L(q - q^*)$ at the surface, 850 mb, 700 mb, 500 mb, 400 mb, 300 mb, 250 mb, 200 mb and 150 mb, and the mean values of $-\partial h^*/\partial z$ for the layers between these levels were used. The correlation coefficients are 0.934 for the first component and 0.826 for the second component.

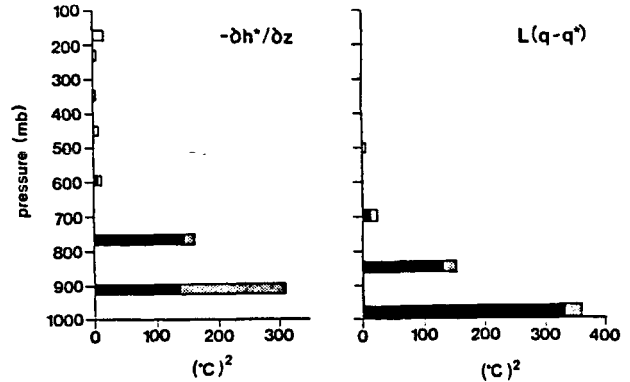


Fig. 1. Accumulated variances of $-(\partial h^*/\partial z) \times 2$ km and $L(q - q^*)$ for the Asian dataset. The solid and stippled bars represent the contributions from component 1 and 2, respectively. The unit is equivalent to $^{\circ}\text{C}$ when divided by c_p .

Figure 1 presents the accumulated variances of $-\partial h^*/\partial z$ and $L(q - q^*)$ at each level (or for each layer). A striking feature of this figure is that large variances are almost entirely due to the two highly-correlated components. This indicates that the type I coupling is very strong. Figure 2 presents the vertical structure of the deviations from the sample mean due to each component. When the deviation of $L(q - q^*)$ due to the first component is positive (relatively moist) at

the surface, as in the figure, that of $-\partial h^*/\partial z$ is negative (relatively stable) for the layer above. This is consistent with the result of the "quick-look" analysis. In contrast to the first component, the second component has a finer vertical structure for both $-\partial h^*/\partial z$ and $L(q - q^*)$. Since components 1 and 2 have no correlations, the structures of components 1 and 2 can be either positively superposed or negatively superposed. When positively superposed, the vertical structures are more confined near the surface for both $-\partial h^*/\partial z$ and $L(q - q^*)$ than the case of component 1 alone; the opposite is true when negatively superposed.

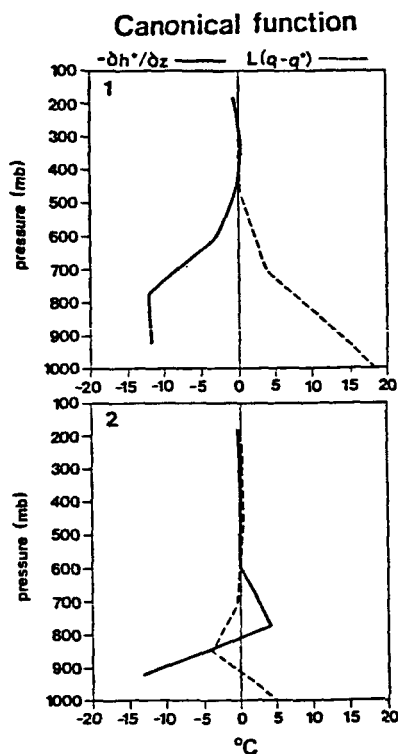


Fig. 2. Vertical structure of the deviations of $-(\partial h^*/\partial z) \times 2 \text{ km}$ (solid lines) and $L(q - q^*)$ (dashed lines) from the sample mean due to one standard deviation of each component.

Type II coupling

For the GATE dataset, $Q_1 - Q_R$ and Q_2 were chosen as X and Y. The correlation coefficients are 0.947 for the first component, 0.736 for the second component, and 0.651 for the third component. For the Asian dataset, Q_1 and Q_2 are chosen as X and Y. The correlation coefficients are 0.845 for the first component, 0.324 for the second component, and 0.095 for the third component. It is not clear whether the lower correlations for the Asian dataset are due to poor data quality, including errors in computed ω , or due to the use of Q_1 instead of $Q_1 - Q_R$, or due to differences in physical situation between the two regions.

Figures 3 and 4 present the accumulated variances for the GATE and Asian datasets, respectively. Although it is not as striking as for the type I coupling, we see from these figures that large total variances are mainly due to the highly-correlated components.

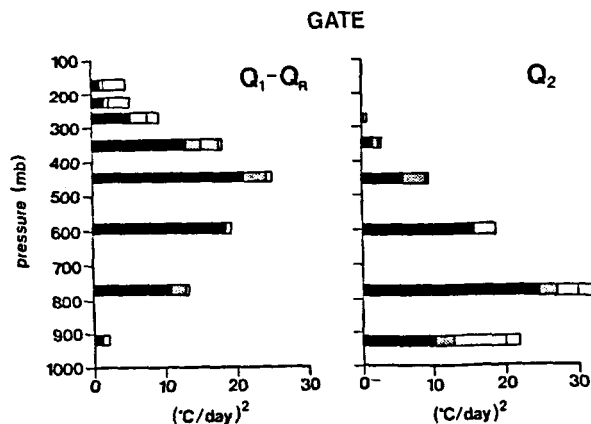


Fig. 3. Accumulated variances of $Q_1 - Q_R$ and Q_2 for the GATE dataset. The solid, darkly-stippled and lightly-stippled bars represent contributions from components 1, 2, and 3 respectively. The unit for $Q_1 - Q_R$ and Q_2 is equivalent to $^\circ\text{C day}^{-1}$ when divided by c_p .

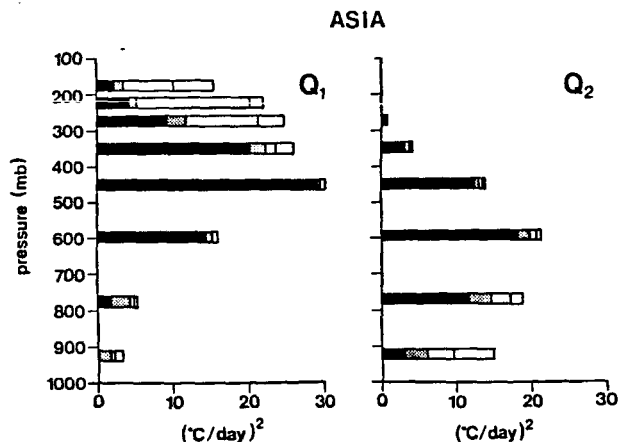


Fig. 4. Same as Fig. 3 but for Q_1 and Q_2 for the Asian dataset.

Figure 5 presents the vertical structure of the deviations from the sample mean due to each component. We can interpret different superpositions of these components as different regimes of moist-convective processes. We note that, in spite of the differences in correlation coefficients, the vertical structures for each component are very similar between the two datasets. Generally the maxima and minima for the Asian dataset appear at higher levels than for the GATE dataset. This is presumably due to generally higher cloud bases for the Asian dataset.

3. RESULTS WITH HIGH VERTICAL RESOLUTION

We are continuing the canonical correlation analysis for type I and type II coupling, but using the data with higher vertical resolution. The dataset we are now using for type I coupling is the VIMEX dataset (see Betts and Miller, 1975) for a single station in north-central Venezuela for the period of 22 May through 6 September, 1972. The vertical resolution of 25 mb is used for the analysis, although the interval 100 mb is used for calculating $\partial h^*/\partial z$. The dataset we are using for type II coupling is the GATE dataset with the original vertical resolution used by Ooyama, Esbensen and Chu.

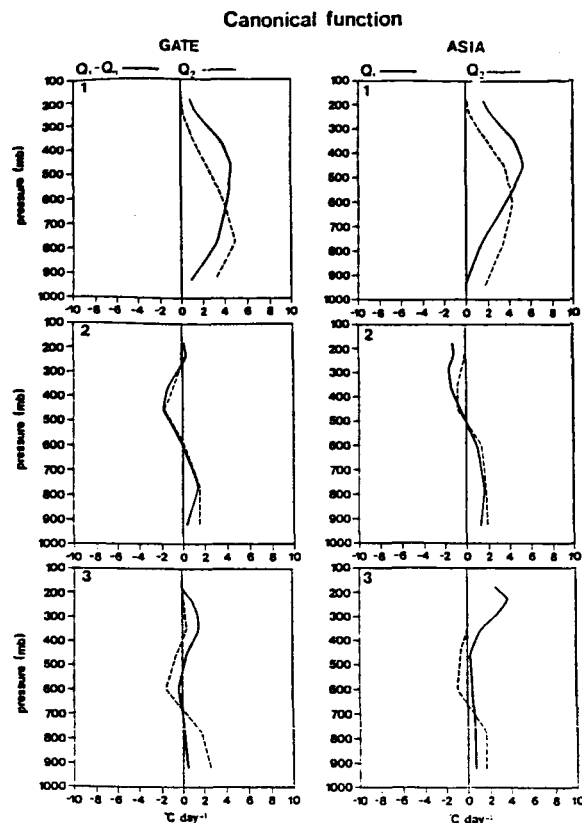


Fig. 5. Vertical structure of $Q_1 - Q_R$ or Q_1 (solid lines) and Q_2 (dashed lines) from the sample mean due to one standard deviation of each component. Left and right panels are for the GATE and Asian datasets, respectively.

The correlation coefficients for the type I coupling with the VIMHEX dataset are 0.980 for the first component, 0.766 for the second component and 0.665 for the third component. We have found that most of the variances are due to these three components. This indicates that the type I coupling is strong also for this dataset. The vertical structures due to the first and second components are similar to those shown in Fig. 2, although the vertical extent of the first component is shallower for this dataset.

The correlation coefficients for the type II coupling for a 10×10 grid box with the high-resolution GATE dataset are 0.928 for the first component, 0.747 for the second component and 0.484 for the third component. Figure 6 presents the accumulated variances showing that the large total variances are mainly due to these components. Figure 7 presents the vertical structures of the deviations from the time mean due to each of the first and second components. These structures are similar to those shown in Fig. 5 except that the deviation of Q_2 due to the second component is larger at lower levels. We are currently analyzing the time sequences of these components and interpreting the result in view of the processes that are responsible for Q_1 and Q_2 .

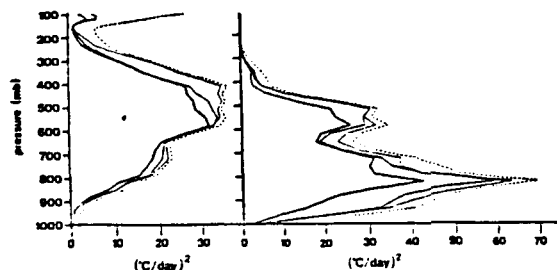


Fig. 6. Same as Fig. 3 but with the high-resolution GATE dataset. The dashed lines show the total variance.

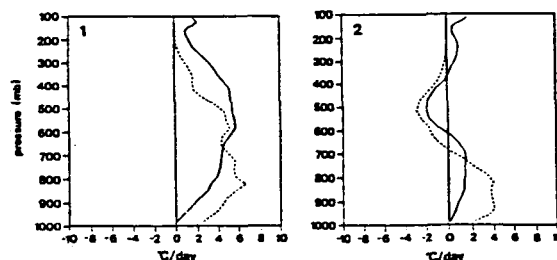


Fig. 7. Same as Fig. 5 but for the first and second components with the high-resolution GATE dataset.

ACKNOWLEDGEMENT

This material is based upon work supported jointly by the NSF and NOAA under Grant ATM-8515013 and by NASA under Grant NAG 5-789.

REFERENCES

- Arakawa, A., and W. H. Schubert, 1974: Interaction of a cumulus cloud ensemble with the large-scale environment. Part I. *J. Atmos. Sci.*, **31**, 674-701.
- _____, and J.-M. Chen, 1987: Closure assumptions in the cumulus parameterization problem. To be published in a special volume of *J. Met. Soc. Japan*.
- Betts, A. K., and R. D. Miller, 1975: VIMHEX-1972 rawinsonde data. Atmos. Sci. Res. Report, Colorado State University.
- Cooley, W. W. and P. R. Lohnes, 1971: Multivariate Data Analysis. Wiley, New York, pp. 364.
- Cox, S. K., and K. T. Griffith, 1979: Estimates of radiative divergence during Phase III of the GARP Atlantic Tropical Experiment: Part I, Methodology. *J. Atmos. Sci.*, **36**, 576-585.
- Esbensen, S. K., and K. V. Ooyama, 1983: An objective analysis of temperature and relative humidity data over the B and A/B ship arrays during Phase III of GATE. Department of Atmospheric Sciences, Oregon State University. 87 pp.
- He, H., M. Yanai and J. W. McGinnis, 1986: The effects of the Tibetan Plateau on the Asian summer monsoon of 1979. To be published.